GAS BUBBLE GROWTH AND DETACHMENT UNDER REDUCED GRAVITY

G. M. Gladchenko, Yu. A. Kirichenko, and K. V. Rusanov

UDC 536.423.18

Helium bubble growth and detachment are considered in liquid oxygen subject to variations in acceleration and hole diameter.

The phase interactions for a gas (vapor) bubbling into a liquid are governed by various factors. Universal formulas have been proposed [1] for the bubble detachment diameter D_d, the time of growth to detachment τ_d, and the mean growth rate $W = D_d/\tau_d$ for a wide pressure range. It is of interest to check those formulas when another factor varies: the acceleration. For convenience, it is best to reduce the acceleration g from the terrestrial gravitational acceleration g_n (i.e., load factor $\eta = g/g_n \leq 1$) because for $\eta > 1$ in a centrifugal system [2, 3], the pressure at the exit from the bubbler hole is a function of η, and it is fairly difficult to define how the latter affects D_d, τ_d, and W in pure form.

We have simulated reduced gravity by partial compensation by means of a magnetic force acting on a liquid paramagnetic (oxygen) in an inhomogeneous magnetic field [4]. The pole tip configuration [5] provides the field in an SP-47 direct-current magnet. Here η is related to the field strength and susceptibility X of the oxygen by

$$\eta = 1 - \frac{X}{2g_n} |\text{grad}\, H^2| \tag{1}$$

or

$$\eta = 1 - (H/H_0)^2, \tag{2}$$

in which H_0 is the field strength corresponding to $\eta = 0$. An estimate [4] is that the error in the simulation is not more than $\Delta\eta = 0.01$.

Equation (1) can be derived from the expression for the sum of the mss forces (gravitational force ρg_n and magnetic force), which act in opposite directions on unit volume of the liquid oxygen, which has density ρ and is placed in the magnetic field:

$$\rho g = \rho g_n - \frac{X}{2} |\text{grad}\, H^2|, \tag{3}$$

in which ρg is the resultant force and $X = \chi/\rho$.

By integrating (1), (2) is derived. If one assumes that in the pole tip symmetry plane (in Fig. 1, in the plane corresponding to the middle of gap and perpendicular to the plane of the figure), the magnetic field is dependent only on the coordinate x reckoned along the vertical axis, i.e., $|\text{grad}\, H^2| = d/dx\,(H^2)$, then

$$H^2 = 2g_n(1-\eta)\,x/X, \tag{4}$$

from which (2) follows.

Weak mass-force fields have been simulated by means of an inhomogeneous magnetic field (in a solenoid) in researching oxygen boiling [6]. The basis for (1) and (2) has been given in [4-6].

The [4] method of simulating small gravitational accelerations has been used [7] to examine vapor bubbles in oxygen at atmospheric pressure; in [8], results were given from similar experiments over a wide pressure range.

Low-Temperature Technical Physics Institute, Ukrainian Academy of Sciences, Kharkov.
Translated from Inzhenerno-Fizicheskii Zhurnal, Vol. 58, No. 2, pp. 190-196, February, 1990. Original article submitted October 18, 1988.

0022-0841/90/5802-0137$12.50

Low gravity is simulated for bubbling (boiling) in the realization not of η for the liquid but of η_g for gas (vapor) bubbles having density ρ_g [4, 6]:

$$\eta_g = \eta + (1-\eta)\frac{\rho g}{\rho - \rho_g}\frac{X - X_g}{X}. \quad (5)$$

The systematic error in the gravity simulation $\Delta\eta_g = \eta - \eta_g$ (for helium bubbles in oxygen $\Delta\eta_g \approx 1.54\cdot10^{-2}$) can be neglected if one defines the state of weightlessness (where $\Delta\eta_g$ is maximal) and the corresponding magnetic field H_0 from the indifferent position of a vapor bubble and calculates the acceleration from (2).

The pole tips were designed for a minimum air gap of 65 mm between the poles and for a maximum field H_0 = 13 kOe.

It has been found [9, 10] that increasing the strength of a homogeneous magnetic field from zero to 57.2 kOe reduced D_d in water boiling, where it was considered that this was due to change in the contact angle θ from 75° at H = 0 to 50° at 57.2 kOe as a result of the field, which corresponds to Fritz's formula relating D_d and θ:

$$D_d = 0.02\theta[\sigma/g(\rho - \rho_g)]^{1/2}, \quad (6)$$

in which σ is surface tension.

The contact angles are small for cryogenic liquids, and in particular $\theta \approx 0$ for oxygen on glass and steel, or 1.5° on platinum or about 7° on teflon [11, 12]. Therefore, vapor bubbles detach in the quasistatic state for sufficiently large d (hole diameter) not from the wall in accordance with (6) but from the edges of the hole, where the detachment diameter is described by Krevelen's formula [13] and is independent of θ [12, 14]. Our range in H was less by a factor of almost five than that in [9, 10], so the theoretically possible variation in θ in the field does not influence the detachment.

We examined bubbles entering liquid oxygen for $\eta = g/g_n$ = 1-0.01. The incoming gas was helium, which does not condense at the boiling point of oxygen. The field strength in the working zone was recorded with an E 11-3 induction meter.

Figure 1 shows the apparatus. The main part is the cryostat in the pole gap in the electromagnet 1. The helium is supplied from the cylinder 2 via the reducing and control valve 3 along a pipe having an internal diameter of 8 mm and total length about 3 m in the cryostat. The working volume in the cryostat 4 is filled via the bellows 5 with liquid oxygen (about 5 liters). Helium passes through the liquid along the copper spiral 6 having internal diameter 4 mm and length 1950 mm and is cooled to the boiling point of oxygen (90 K). At the lower end of the coil opposite the cryogenic optical illuminators 8 there is the bubbler 7; the bubbles are observed without external perturbation because the bubbler is placed in the gas cylinder having diameter 35 mm. The bubbler consists of a PTFE cylindrical body with interchangeable capillaries placed vertically at the upper end, which has a diameter of 20 mm. The upper ends of the capillaries are not especially worked. We used capillaries having internal diameters d of 0.58, 1.01, and 2.21 mm and outside diameters of 0.83, 1.23, and 2.93 mm correspondingly. In the first series, the capillaries projected above the body

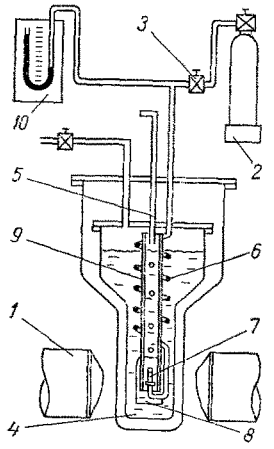

Fig. 1. The apparatus.

correspondingly by 4.0, 6.0, and 10.0 mm, while in the second series, the upper ends were level with the horizontal end of the body. In the working volume, i.e., at the capillary exits, the pressure was atmospheric. The excess pressure in the injection line was kept constant at 200 mm of oil and was monitored with the U-tube manometer 10. The low excess pressure meant that the gas emerged only as bubbles, which grew fairly slowly. The height of the liquid column above the upper end of a capillary was 120-150 mm.

Illumination was provided by a 500 W lamp. Cinematography was provided by an SKS-1M camera with Jupiter-6 lens, speed 500 to 2000 frames a second. The films were examined with a Mikrofot to determine two bubble dimensions: vertical a and horizontal b, with the scale provided by the capillary itself, which had a known outside diameter. The equivalent bubble diameter was calculated as $D = (a + b)/2$. The relative errors in determining a and b were 30-50% at the start of growth but 3-8% at detachment. The error in determining τ was governed by the recording speed and was $(0.25\text{-}2) \times 10^{-3}$ sec.

The detachment instant was determined from the occurrence of a band of liquid between the bubble and the end of the capillary. The time from the start of bubble growth to detachment was considered as the growth time τ_d, while the interval between detachment and the production of the next bubble was taken as the waiting time τ_w.

As in boiling, gas bubble growth is described by

$$R = \beta\tau^n, \tag{7}$$

in which R is current radius and β the growth modulus [12]; n is very slightly dependent on η and d. For $0.01 \leq \eta \leq 1$, series 1 gave

$$n = 0.492\eta^{0.022}. \tag{8}$$

This agrees well with the [14] result for bubbling and boiling with $\eta = 1$:

$$n \sim (d/B)^{0.04}, \tag{9}$$

in which $B = [\sigma/g(\rho - \rho_g]^{1/2}$ is the Laplace constant.

The growth modulus is dependent on the acceleration and diameter more than is n:

$$\beta = C\eta^k, \tag{10}$$

in which C = 12.8; 16.9; 17.0 mm/sec^n and k = 0.14; 0.14; 0.094 for d = 0.58; 1.01; 2.21 mm, correspondingly. The data for $\eta < 1$ implies $\beta \sim d^{0.22}$.

We estimated the forces acting on the bubble during growth by the [12] method; there was always quasistatic growth and detachment.

Figure 2 shows the detachment size as a function of acceleration, where each point has been obtained by averaging from 5 to 30 D_d. That diameter decreases as d falls and as η increases. The lines in Fig. 2 are from the formula [1]

$$D_d = A\frac{d}{2}\left(\frac{2B}{d}\right)^{2/3}\left(\frac{\rho - \rho_g}{\rho_g}\right)^{1/8}, \tag{11}$$

in which A = 1.58. Data fitting gave A = 1.023 for series 1 and A = 1.132 for series 2; the standard deviations of the measurements from the lines were from 10 to 17%. With a projecting capillary, D_d on average was somewhat less than in series 2.

Equation (11) differs from Krevelen's formula [13]

$$D_d = C_1\left[\frac{6\sigma d}{g(\rho - \rho_g)}\right]^{1/3}, \quad C_1 \approx 1, \tag{12}$$

in the factor $\sqrt[8]{(\rho - \rho_g)/\rho_g}$ and describes the measurements with about the same accuracy. The measured D_d fit (12) satisfactorily with $C_1 = 1.10$ for series 1 and $C_1 = 1.25$ for series 2. The standard deviation did not exceed 20% for each series.

A formula proposed for the growth time [1] is

$$\tau_d = A_1 \mathrm{Pr}^{-1/2}\frac{d}{2}\left(\frac{\rho - \rho_g}{P}\right)^{1/2}\left(\frac{\rho - \rho_g}{\rho_g}\right)^{1/8} \times \left[\frac{P^2}{g\sigma(\rho - \rho_g)}\right]^{2/5}\left(\frac{2B}{d}\right)^{2/3}, \tag{13}$$

in which Pr is the Prandtl number for the liquid, P is pressure, and $A_1 = 0.118$. Figure 3 compares our measurements with (13). For series 2, $A_1 = 0.088$, and for series 1, $A_1 = 0.118$,

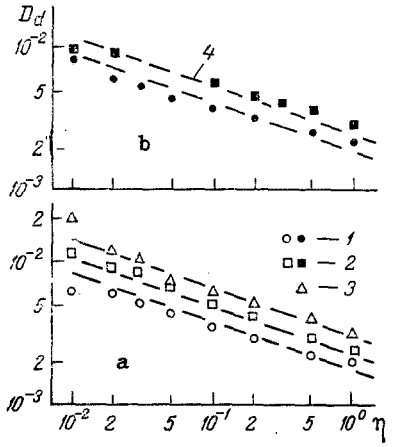

Fig. 2. Detachment diameter as a function of acceleration: 1) d = 0.58; 2) 1.01; 3) 2.21 mm; 4) from (11); a) series 1 data; b) series 2. Diameters in m.

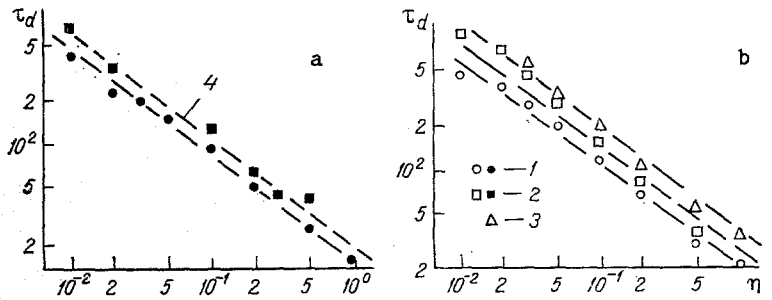

Fig. 3. Bubble growth times in msec as functions of acceleration: 1-3) see Fig. 2; 4) from (13); a) series 1 data; b) series 2.

which agrees with the [1] conclusion. For d = 0.58; 1.01; 2.21 mm, the standard deviations from (13) were 11, 24, and 12%.

Equations (11) and (13) reflect satisfactorily not only how d and P affect the detachment characteristics but also the effects of g: $D_d \sim \eta^{-1/3}$; $\tau_d \sim \eta^{-11/15}$. The measurements give the exponent in the D_d formula as on average 0.32, and that for τ_d as 0.79, which are very close to the values in (11) and (13).

Table 1 also gives some other characteristics. The waiting time shows a spread even in the mean values much larger than that for τ_d. In some experiments, there was no waiting period. However, it is evident that τ_w decreases as the acceleration rises, and to a first approximation, $\tau_w(\eta)$ is close to that for the growth time; there is no single-valued effect from the hole diameter on the waiting time. Figure 3 and the τ_w data indicate that the growth time is long by comparison with the waiting one, and τ_w/τ_d only in three cases out of 36 exceeded 0.2, so the effects of η and d on the detachment frequency $f = 1/(\tau_d + \tau_w)$ are determined in the main by the τ_d dependence on the acceleration and hole diameter; on average $f \sim \eta^{0.77}$; $f \sim d^{-0.40}$.

The shape on detachment is characterized by the skewness coefficient b/a. For η = 0.5-1, the bubbles are almost spherical, but as the acceleration decreases, the bubbles gradually become elipsoids with axis ratio about 1.5. Here $b/a \sim \eta^{-0.065}$. As small accelerations correspond to strong fields in (2), the deformation is presumably caused by the transverse magnetic force acting on the phase boundary perpendicular to the recording direction. Increased deformation at low η is facilitated by the considerable detachment sizes: the surface-tension forces opposing sphericity deviation are inversely proportional to D_d.

If a bubble is an ellipsoid having the long horizontal axis b, the volume is $v = \pi a^2 b/6$. Then for b/a = 1.5, the real equivalent diameter D_d is about 9% less than (a + b)/2,

TABLE 1. Waiting Time, Detachment Frequency, and Skewness Coefficient with Varying Acceleration Varying Acceleration for Various Hole Diameters

η	d=0,58 mm		d=1,01 mm		d=2,21 mm
	series 1	series 2	series 1	series 2	series 1
	$\tau_w \cdot 10^{-3}$, sec				
0,01	31,4	87,5	0	24,4	—
0,02	17,3	67,9	51,1	26,4	—
0,03	9,5	37,1	17,6	—	7,0
0,05	13,8	13,0	74,2	—	16,9
0,1	6,9	2,4	17,8	3,8	7,7
0,2	3,6	2,5	11,8	0,8	3,8
0,5	1,3	1,7	5,9	0,9	1,8
1,0	0,6	1,0	0	0	2,2
	f, sec^{-1}				
0,01	2,11	2,22	1,16	1,46	—
0,02	2,60	3,31	1,38	2,49	—
0,03	3,61	4,24	2,16	—	1,76
0,05	4,76	6,39	2,76	—	2,91
0,1	8,36	10,9	6,02	7,82	4,94
0,2	14,4	18,4	10,5	15,4	9,28
0,5	29,6	37,0	23,7	23,4	17,9
1,0	47,8	62,3	38,5	47,8	27,0
	b/a				
0,01	1,25	1,50	1,67	1,41	1,46
0,02	1,44	1,37	1,58	1,48	1,46
0,03	1,41	1,37	1,57	—	1,38
0,05	1,32	1,29	1,47	—	1,36
0,1	1,26	1,18	1,29	1,21	1,21
0,2	1,16	1,15	1,18	1,11	1,18
0,5	1,12	1,03	1,12	1,07	1,11
1,0	1,04	1,02	1,16	—	1,09

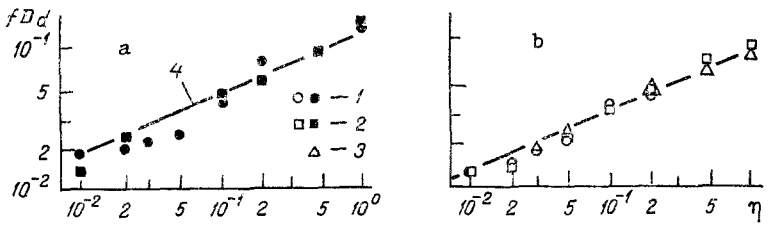

Fig. 4. Mean growth rate as a function of acceleration: 1-3) see Figs. 2 and 3; 4) from (14); a) series 1; b) series 2 (values in m/sec).

which is within the usual spread in the repeat measurements on a given film. The distortion unimportant in quasistatic growth may however have an appreciable effect on the subsequent rise.

The mean growth rate $W = D_d/\tau_d = fD_d$ is [1] given by

$$W = A_2 \mathrm{Pr}^{1/2} [P/(\rho - \rho_g)]^{1/2} \left[\frac{g\sigma(\rho - \rho_g)}{P^2}\right]^{2/5}, \quad (14)$$

in which $A_2 = 13.3$.* The value W is thus independent of the hole diameter, and the dependence on the acceleration is $W \sim \eta^{2/5}$. Both these conclusions [1] agree well with out results (Fig. 4). On average, the measurements give $W \sim \eta^{0.46}$, with $A_2 = 8.49$ for series 1 and $A_2 = 12.2$ for series 2 with standard deviations of 12 and 21% correspondingly.

These early measurements on gas bubble growth and detachment from a single hole at η of 0.01-1 show that the formulas proposed by Malenkov et al. reflect satisfactorily the effects of the acceleration on the bubble detachment characteristics.

*In [1] the exponent with the last cofactor was erroneously written as 0.5.

LITERATURE CITED

1. I. G. Malenkov, D. A. Vezirishvili, and E. A. Chinnov, Boiling and Condensation: Hydrodynamics and Heat Transfer [in Russian], Novosibirsk (1986), pp. 13-23.
2. N. M. Levchenko and I. M. Kolod'ko, Thermal Processes in Cryogenic Systems [in Russian], Kiev (1986), pp. 45-47.
3. A. I. Safonov and V. S. Krylov, Heat and Mass Transfer V [in Russian], Minsk (1976), Vol. 4, pp. 85-93.
4. Yu. A. Kirichenko, A. I. Charkin, I. V. Lipatova, and V. L. Polunin, Inzh.-Fiz. Zh., 17, No. 2, 201-210 (1969).
5. M. Garber, W. G. Henry, and H. G. Hoeve, Can. J. Phys., 38, No. 12, 1595-1613 (1960).
6. D. N. Lyon, M. C. Jones, G. L. Ritter, C. I. Chiladakis, and P. G. Cosky, AIChE J., 11, No. 5, 773-780 (1965).
7. Yu. A. Kirichenko and A. I. Charkin, Heat Transfer 1970, Proc. 4th Int. Heat Transfer Conference, Paris–Versailles, 1970, Elsevier, Amsterdam (1970), Vol. 6, Paper B 8.9.
8. Yu. A. Kirichenko and G. M. Gladchenko, Hydromechanics and Transport Processes under Zero Gravity [in Russian], Sverdlovsk (1983), pp. 72-85.
9. N. B. Chigarev and T. S. Chigareva, Inzh.-Fiz. Zh., 41, No. 2, 209-213 (1981).
10. N. B. Chigarev, Inzh.-Fiz. Zh., 46, No. 5, 721-723 (1984).
11. W. B. Bald, Cryogenics, 13, No. 8, 457-469 (1973).
12. B. I. Berkin, Yu. A. Kirichenko, and K. V. Rusanov, Heat Transfer in Cryogenic-Liquid Boiling [in Russian], Kiev (1987).
13. D. V. Krevelen and P. J. van Hoftijzer, Chem. Eng. Progr. Symp. Ser., 46, No. 1, 29-35 (1950).
14. N. S. Shcherbakova, A Study on the Mechanisms of Quasistatic Bubble Growth and Detachment in Application to Bubbling and Boiling: Ph. D Thesis [in Russian], Kharkov (1983).

DIMINUTION OF THE THERMAL ACTION OF A GAS JET ON A PLATFORM BY DELIVERY OF COOLANT IN THE NEIGHBORHOOD OF THE CRITICAL POINT

N. I. Melik-Pashaev,* É. K. Moroz, and A. I. Mel'nikov

UDC 532.525.6

Results are presented of an experimental investigation of the thermal action of a high-enthalpy jet on a normally disposed platform and the means to diminish this effect.

The thermal action of a gas jet impinging on a normally disposed platform can be diminished by supplying coolant in the neighborhood of the critical point [1]. Investigations were performed on an experimental installation including an axisymmetric nozzle through which a preheated gas escaped onto the platform model (Fig. 1). The platform models were an asbestos-plastic slab and a steel plate with installed thermocouples to measure the gas flow temperature near the platform surface T_g^* and the platform surface temperature T_w. The models were moreover equipped with sensors to measure the heat flux density q by the auxiliary wall method [2, 3] and by alpha-calorimeters to measure the heat elimination coefficients by the α method of a regular thermal mode [2, 4]. The temperature T_g^* was measured near the surface when using the asbestos-plastic slab, however, because of the low heat conductivity of the slab this quantity is close to the wall temperature T_w. Measurement of the temperature T_{cool} and the mass flow rate G_{cool} of sprayed in water or blown-in air was provided for in the neighborhood of the critical point in the coolant delivery mainlines.

*Deceased.

Translated from Inzhenerno-Fizicheskii Zhurnal, Vol. 58, No. 2, pp. 197-199, February, 1990. Original article submitted October 18, 1988.

 0022-0841/90/5802-0142$12.50